doi.org/10.36721/PJPS.2021.34.3.SUP.1119-1126.1

Development of potent remdesivir derivative against SARS-CoV-2 protease inhibitors: Design, modification, molecular modeling and MD simulations

Mahwish Akhtar[1] and Sumbul Shamim[2]*

[1]Department of Pharmaceutical Chemistry, Faculty of Pharmaceutical Sciences, Dow College of Pharmacy, Dow University of Health Sciences, Karachi, Pakistan

[2]Department of Pharmacology, Faculty of Pharmaceutical Sciences, Dow College of Pharmacy, Dow University of Health Sciences, Karachi, Pakistan

Abstract: The pandemic Coronavirus (Covid-19) is continuously growing and spreading at the highest rate in all over the world. So, it is necessary to produce the new medicinal agents against this virus. The aim of the present study is to design a potent compound against COVID-19. Based on 3C-like main protease and recently developed solved structure (PDB ID: 6Y2F), a series of remdesivir analogs are designed and analyzed by employing molecular modeling against the SARS-CoV-2 by *insilico* approach. The molecular dynamics (MD) simulation for 500ps was performed to check the stability and orientation to inside the binding pocket for analogs R3, R9, R14 and R15. The study results exhibit that compsound R9 has strong interaction or least binding energy (-10.04kcal/mol) as compare to the other analogues due to the presences of methyl bromide and it may be useful to further investigation *in vitro* testing against Covid-19.

Keywords: SAR-CoV-2, 3C-like protease, remdesivir, docking study, drug designing.

INTRODUCTION

The official name of novel coronavirus is severe acute respiratory syndrome coronavirus 2 (SARS-CoV-2). It was first reported in Wuhan city China in late 2019 and rapidly spread all over the world till March 2020 (Cao Y *et al.,* 2020). Recently the scientists have taken fast actions, against COVID-19, to isolate the virus, evaluate the gene sequence and identify the treatment (Kumar *et al*., 2020). It was reported that coronavirus belongs to the Beta-Coronavirus. The life cycle in the host cell is divided in to following steps: 1) translation of genomic RNA (gRNA), 2) proteolysis of the translated poly protein with viral 3C-like proteinase (Mpro), 3) replication of gRNA with the viral replication complex that consists of RNA dependent RNA polymerase (RdRp), helicase, 30-to-50 exonuclease, endoRNAse and 20-O-ribose methyl transferase and 4) assembly of viral components (Fung, *et al.,* 2019). The Mpro is further divided into three main domains; the first domain consist of 8 to 101 amino acid residues, the second domain contain 102 to 184 amino acid residues and the third domain comprise of 185 to 200 amino acid residues. The first and second domain demonstrates chymotrypsin catalytic domain and third domain represents helical structures which participate in dimerization of protein and active enzyme production (Bacha *et al.,* 2004*, Zang et al.,* 2004). Unlike other viral proteases, Mpro uses Cys residue of the catalytic dyad instead of Ser residue for nucleophilic attacks (Bacha *et al.,* 2004; Anand *et al.,* 2002) due to this Mpro is considered as right active site for virus inhibition.

The S-protein of SARS-CoV-2 binds with the ACE2 receptor by 4 to 5 specific amino acids (Xu *et al.,* 2020) and it has been reported that the binding affinity of coronavirus is approximately 10-20 times greater than the SARS (Wrapp *et al.,* 2020).

Previously, the patients of SARS and MERS were treated with lopinavir, interferon, ribavirin and corticosteroids (Wang *et al.,* 2020), within the selection range of "conventional drug in new us". Earlier, remdesivir was used as a potent anti-viral agent for the treatment of MERS-CoV. Now remdesivir (referred as RDV) (fig. 1) is successfully used against COVID by inhibiting the replication of virus in respiratory epithelial cell. The first patient recovered from COVID-19 with the in 24 hours treatment of RDV was from United States (Cao Y *et al.,* 2020).

RDV is a prodrug of an adenosine analogue which is used against RNA virus category and nowadays, it is utilized against SARS-CoV-2 (Sheahan et al., 2020; Pizzorno et al., 2020; Williamson et al., 2020). It is the inhibitor of RNA synthesis and active against RNA viruses (Al-Tannak NF *et al.,* 2020) and recently, RDV is shown to inhibit SARS-CoV-2 viral replication in cell culture, (Wang *et al.,* 2020). Owing to this tendency, RDV is selected as the target drug for *insilico* study for the inhibitor of RNA dependent RNA polymerase (RdRp) (Elfiky *et al.,* 2020, Shannona *et al.,* 2020, Koulgi *et al.,* 2020, Elfiky *et al.,* 2020).

Our aim is to predict a potent molecule for the treatment of corovirus by this way we can save the important human

**Corresponding author:* e-mail: sumbul.shamim@duhs.edu.pk

life. To achieve this goal, we selected this antiviral drug molecule of RDV, showing activity against SARS-CoV-2. Using this molecule we designed a series of novel derivatives of RDV, converted it into 3D structure then minimized their energies and produced PDB file for further study. The computationally designed analogs were screened against the recently isolated protein of coronavirus i.e Mpro by molecular docking. The results of analogs were compared with the parent lead molecule that was RDV as well as with the ligand of protein that was α-ketoamide. In future, we will perform the *invitro and in vivo* study to verify the *insilico* results.

MATERIALS AND METHODS

Designing of analogs

After the Structure Activity Relationship study of RDV (Eastman *et al.,* 2020, Al-Tannak *et al.,* 2020) the primary amine group of the drug was selected to generate a series of analogs. The 2D structures of RDV, ligand (α-ketoamide) and designed derivatives were drawn on Marvin-Stretch Version 5.5 are licensed software and structures were saved in SDF format also (table I).

Preparation of protein

The recently discovered crystal structure of SARS-CoV2 (PDB ID-6Y2F) (Zhang *et al.,* 2020) was selected to construct the predictive model for the designed analogs series of RDV. The protein structure was downloaded from RCSB-PDB with a resolution of 1.95 Å (http://www.rcsb.org/pdb/home/home.do). The protein structure was already complex with α-ketoamide 13b. The complex ligand (α-Ketoamide) and solvent molecules were removed from the selected PDB file using Discovery Studio and the polar hydrogen and Kollman united atom charges were introduced in PDB file using the AutoDock program.

Preparation of inhibitor

The 3D structures of designed analogs were created on ChemDraw 4D ultra (Version 16.0) (Chemical Structure Drawing Standard; Cambridge Soft Corporation, USA (2009)). The hydrogen atoms were introduced. MMFF94X force-field method was used to minimize energies of all analogs. Furthermore, all analogs were converted into PDB format. The MGL Tools (version 1.5.6) (Trott, *et al.,* 2010) were used to generate PDBQT files. This conformation was allowed to analogs for the flexible molecular docking process.

Molecular docking

The docking program AutoDock (version 1.5.6) was used to perform the automated molecular docking. The Lamarckian genetic algorithm (LGA) was applied to deal with the inhibitor-enzyme interactions. The grid box was produced in the center of active site domains of M^{pro} including Leu^{27}, His^{41}, Cys^{44}, Thr^{45}, Met^{49}, Phe^{140}, Leu^{141}, Asn^{142}, Gly^{143}, Ser^{144}, Cys^{145}, Glu^{163}, His^{164}, Met^{165}, Glu^{166}, Leu^{167}, Pro^{168}, His^{172}, Asp^{187}, Arg^{188}, Gln^{189}, Thr^{190} and Gln^{192}. The grid map with 40. 52. 56 points spaced equally at 0.525A° was generated using the AUTOGRID program to evaluate the binding energies between the compounds and the protein. Docking parameters were set to default values for the orientation and torsion angles (7.5), the number of generations (27,000), and the energy evaluations (2500,000). The docked inhibitor–enzyme complexes were ranked according to the predicted binding energies and to the conformity to the ideal geometry of the docked structures.

Screening criteria

The goal of the present research is to identify the best model of analog with the SARS-CoV-2 protein crystal structure. The molecular docking results were visualized and analyzed by using Discovery Studio Visualizer (DS) (BioVia, Discovery Studio Vers. 2.5, San Diego, CA, USA. (2017)), PyMOl molecular visualization tool (PyMOL; The PyMOL Molecular Graphics System, Version 2.0 Schrodinger, LLC) and PLIP (Salentin, *et al.,* 2015).

Molecular dynamic (MD) simulations

The MD simulation analyses were performed for analogs R3, R9, R14 and R15 to check the stability and binding ability with the protein of the SARS-CoV-2 and evaluate the results of the molecular docking analyses. Short MD simulation period was performed for about 500 ps. NAMD 2.14 software package is used to perform the MD simulation analysis using CHARMM 36 force field with map correction (Brooks *et al.,* 2009), with a time-step of 2fs and periodic boundary conditions in all dimensions (MacKerell *et al.,* 1998, Jorgensen *et al.,* 1983). The water molecule is minimized with protein system for 10000 steps each using TIP3P model (Pastor *et al.,* 1988). The temperature was 310K with constant pressure using Langevin piston pressure method and Langevin dynamics temperature (Darden *et al.,* 1996). The particle-mesh Ewald (PME) method was used in the calculation of the electrostatic interactions with 10 Å non-bounded cutoff (Humphrey *et al.,* 1996).

Statistical analysis

The Visual Molecular Dynamic (VMD) program was used for visualization of the structures and trajectories (Humphrey *et al.,* 1996). The trajectories were analyzed by means of backbone RMSD and carbon alpha fluctuations, atom distances. The graph of RMSD and RMSF were generated on MS-Excel (Office 365).

RESULTS

The structures of RDV, ligand (α-ketoamide) are described in fig. 1 and 2 respectively. The derivatives are presented in table 1.

Molecular modelling

The RDV, α-ketoamide and analogs were *in-silico* docked with spike protein of SARS-CoV-2 (PDB ID: 6Y2F). It was observe that all designed analogs were strongly bound with the SARS-CoV-2 as compare to the RDV and some of the analogs (like R3, R9, R14 and R15) were more strongly bound with the target protein as compared to the ligand (α-ketoamide). The free energy of binding (kcal/mol) and inhibition constant (Ki) were available. table 2, fig. 3 and 4 show the binding results of RDV, α-ketoamide and analog R9 respectively.

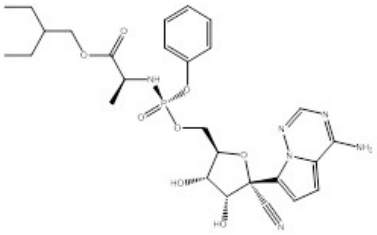

Fig. 1: Remdesivir

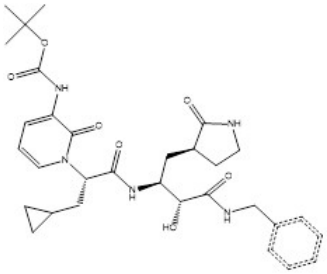

Fig. 2: α-ketoamide

MD Simulation

The interactions of above discussed analogs with PDB-6Y2F were analyzed by the means of RMSD and RMSF. fig. 5 shows the RMSD values of analogs (R3, R9, R14 and R15) for 0.5 ns of time. The energy minimization of each system was analyzed by using steepest decent method of 10000 times. MD simulations with NVT (isochoric-isothermal) and NPT (isobaric-isothermal) ensembles (N¼constant particle number, V¼ Volume, P¼ Pressure, T¼ Temperature) were performed for 0.5 ns to equilibrate the protein-ligand system for constant volume, pressure (1 atm) and temperature (300 K). Particle Mesh Ewald (PME) algorithm (Darden *et al.,* 1993) was used to calculate electrostatic interaction with grid spacing of 1.6Å and a cutoff of 10Å. The trajectories were saved at every 2ps and till 500 ps of production, MD simulation was performed for each system.

DISCUSSION

COVID-19 is a rapidly spreading disease caused by SARS-CoV-2. It was started in late 2019 in Wuhan city of China and spread all over the world. The treatment of COVID-19 is under the process of discovery yet. However, the efforts from the scientific community have been exceptional in advancing research efforts towards the development of therapeutic intervention and finding viral drug targets.

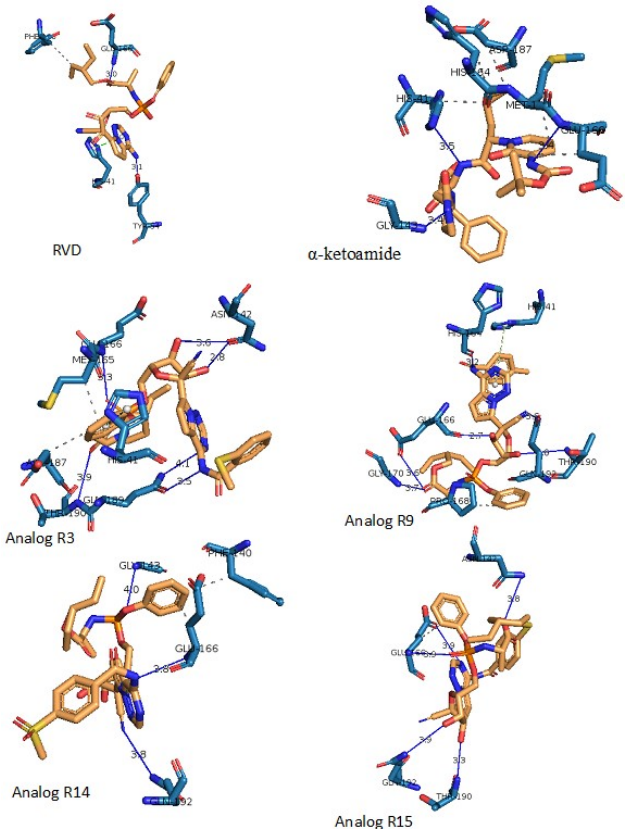

Fig. 3: Schematic of intermolecular interactions of protein and ligand.

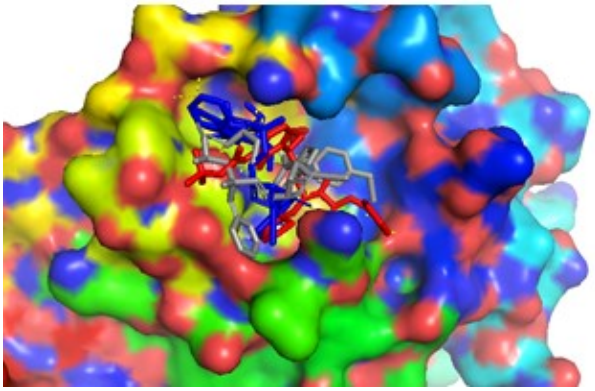

Fig. 4: Molecular docking pose and binding interactions of RDV (blue sticks), (α-ketoamide (red sticks) and R9 (grey sticks) bound to SARS-CoV 3CLpro (PDB ID: 6Y2F).

Structural activity relationship

The binding energies of considered compounds were between -10.08 kcal/mol to -4.71kcal/mol. The RDV is a pro-drug and its structure resembles to the adenosine. The phosphoric acid of RDV is modified by the addition of phenyl and amino substitution. Both substitution were removed during activation. The cyano group at carbon 1

is important for the activity. The above discussed group was not selected for the derivation designing (Al-Tannak NF *et al.,* 2020) and the binding energy of RDV was -4.83 kcal/mol which is considered as poor. The redocking result of ligand that was α-ketoamide with target (PDB id: 6Y2F) was better (-7.36kcal/mol). Nevertheless, the analogs are bound to the target with low to moderate energies. It was observed that the binding energies of all analogs were better than RDV.

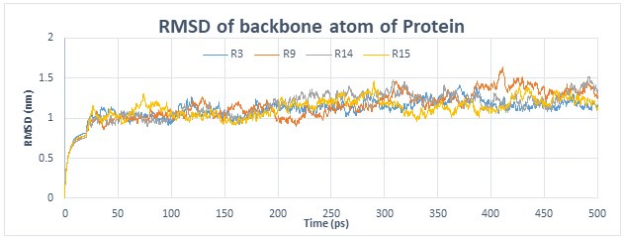

Fig. 5: The root mean square deviation (RMSD) plots for the R3, R9, R14 and R15 compounds interacting with the Mpro protein for the entire 500 ps MD simulation.

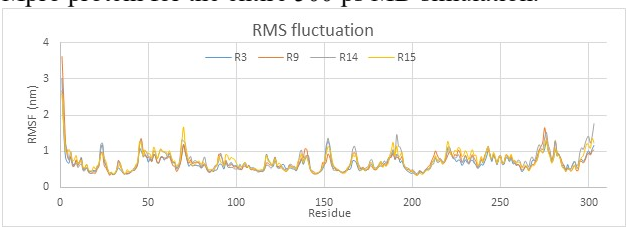

Fig. 6: The RMSF plot for each residue is show over the 500 ps MD simulation.

The primary amine group of pyrrolo[1,2-f][1,2,4]triazin-4-amine of RDV has been selected for the modification. In R1 compound, the hydrogen of primary amine of RDV has been replaced by acetophenone. The binding energy was increased to -5.15kcal/mol. Furthermore, phenyl-methan-amine group was added at the *ortho*-position of acetophenone group of R1. Due to this addition binding energy was further increased to -6.68kcal/mol. Now, sulfur group was added at the *ortho*-position of acetophenone group of R1, the binding energy bacame -8.85kcal/mol. Similarly, three more compounds R4, R5, and R6 were designed by the modification of sulfonyl chloride, tertiary amine and fluoro form at *meta*-position of acetophenone of R1 respectively. The binding energies become moderate that were -6.67kcal/mol for R4,-6.25 kcal/mol for R5 and -5.74 kcal/mol for R6. In compounds R7 to R16, the para position of acetophenone of R1 was selected for modification. In compound R7, 2-chloro-N-methylamide was added at para position of acetophenone, the binding energy was slightly decreased to -6.67 kcal/mol. Similarly, methyl amine, tertiary amine and secondary amine groups were added on R8, R12 and R13 respectively. The binding energies were -4.71 kcal/mol, -5.88 kcal/mol and -5.69 kcal/mol for R8, R12 and R13 respectively. Moreover, with the addition of sulfonyl chloride and methyl sulfonyl group in compound R11 and R14, the binding energies were decreased to -6.06 kcal/mol and -7.51kcal/mol. In R15, methyl sulfur was introduced and the binding energy was decreased to -7.85 kcal/mol. The molecular docking results were observed by the addition of methyl bromide and methyl chloride in compound R9 and R10 respectively. The binding energy of R10 was moderate but compound R9 showed excellent binding energy that was -10.04kcal/mol.

It was observed that by the addition of acetophenone at primary amine of RDV, binding energy increased to -5.15 kcal/mol. Additionally, binding energies of amine containing compounds, R2, R5, R7, R8, R12 and R13, were high to moderate (-4.71kcal/mol to -6.68kcal/mol) and the sulfonyl containing compounds, R4, R11, R14 and R16 were of moderate to low binding energy (-6.06 kcal/mol to -7.51kcal/mol). The sulfur containing compounds, R3 (-8.85kcal/mol) and R15 (-7.85kcal/mol) were of high binding affinities. The binding energies of methyl halide having compounds R6, R9 and R10 were with moderate to low energies (-5.74 to -10.04). The binding energies of R9, R3, R15 and R14 were -10.04 kcal/mol, -8.85kcal/mol, -7.85kcal/mol and -7.51 kcal/mol were better than the α-ketoamide (-7.36 kcal/mol) and they are subjected to further analysis study.

Molecular docking

The process of molecular docking was performed with the default setting. All analogs were ranked according to ascending order of binding energies, it was analyzed by a close study of all 18 compounds listed in table 2. For the results generation, the dlg output file of each compound was run by AutoDock. The clusters of conformations are sorted out according to their RMSD values. All studied compounds have shown zero RMSD value. The binding energies of considered compounds were between -10.08 kcal/mol to -4.71kcal/mol. The binding energy of remdesivir was -4.83 kcal/mol which was considered as high and the binding energy of α-ketoamide was high that is -7.36 kcal/mol. Nevertheless, the binding energies of all most all analogs were better than the selected drug. The analogs are bound to the target with moderate to high energies. The binding energies of R9, R3, R15 and R14 were -10.04kcal/mol, -8.85kcal/mol, -7.85 kcal/mol and -7.51kcal/mol respectively which were better than the α-ketoamide. The ester group of RDV produces hydrogen bonds through the nitrogen of Tyr^{54} with a bond length of 2.70Å and 2.30Å respectively and the terminal nitrogen of RDV attached with the O-atom of Glu^{166}. Additionally, the RDV produced a hydrophobic bond with Phe^{140}. The oxygen atom of the amide group of α-ketoamide makes a hydrogen bond with the oxygen group of His^{41}, Gly^{143}, Glu^{166} and hydrophobic bond with His^{41}, His^{164}, Met^{165}. The R3 analogs produce 6 hydrogen bonds with Asn^{142}, Glu^{166}, Gln^{189}, Thr^{190} and 2 hydrophobic bonds with Met^{165}, Asp^{187}. Among all derivatives the R9 shown the best docking result with the binding energy of -10.04 kcal/mol. It produced a hydrogen bond with His164, Glu^{166}, Gly^{170}, Thr^{190}, Gln^{192} and His^{164}.

Table 1: Designed derivatives of Remdesivir

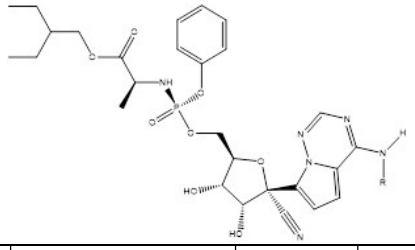

Analogs	Molecular Weight	Molecular Formula	R	Analogs	Molecular Weight	Molecular Formula	R
R1	706	$C_{34}H_{39}N_6O_9P$	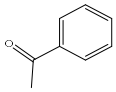	R9	799	$C_{35}H_{40}BrN_6O_9P$	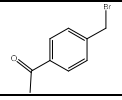
R2	811	$C_{41}H_{46}N_7O_9P$	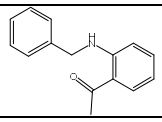	R10	754	$C_{35}H_{40}ClN_6O_9P$	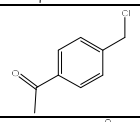
R3	752	$C_{35}H_{41}N_6O_9PS$	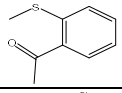	R11	804	$C_{34}H_{38}ClN_6O_{11}PS$	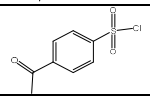
R4	804	$C_{34}H_{38}ClN_6O_{11}PS$	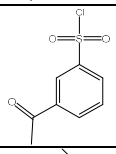	R12	749	$C_{36}H_{44}N_7O_9P$	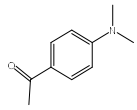
R5	749	$C_{36}H_{44}N_7O_9P$	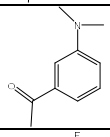	R13	735	$C_{35}H_{42}N_7O_9P$	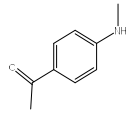
R6	774	$C_{35}H_3F_3N_6O_9P$	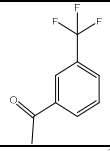	R14	784	$C_{35}H_{41}N_6O_{11}PS$	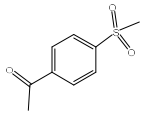
R7	797	$C_{36}H_{41}ClN_7O_{10}P$	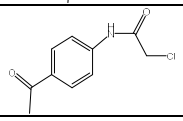	R15	752	$C_{35}H_{41}N_6O_9PS$	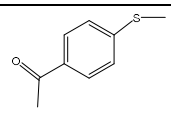
R8	735	$C_{35}H_{42}N_7O_9P$	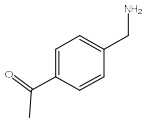	R16	854	$C_{34}H_{38}Cl_2N_7O_{11}PS$	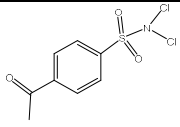

Furthermore, it also creates a hydrophobic bond with Pro[168] shown in table 3. The hydrogen bonds with bond length and hydrophobic interaction of all analogs is compiled and presented in fig. 3. Similarly, analog R14 and R15 produces 4 to 5 hydrogen bonds and 1 to 2 hydrophobic interaction with target protein.

On the bases of above observations the analog R9 were consider as the best compound among all because it shows excellent binding affinity with 6 hydrogen bond which were produce between analog R9 and protein of SARS-CoV2.

Molecular dynamics simulation

The MD simulation study was carried out to evaluate the stability of docking study of ligand-protein complexes. The complexes of protein with analog R3, R9, R14 and R15 were considered for the MD simulation study. The resultant trajectories were analyzed in terms of RMSD (fig. 5) and RMSF (fig. 6).

The stability of each simulation model was estimated by the calculations of backbone atom RMSD for ligand-protein complex. The average value of RMSD of analog R3 was 1.115 nm, R9 was 1.1588 nm, and R14 was 1.1696

Table 2: Docking results of remdesivir analogs

Compounds	Binding Energy (kcal/mol)	Ligand Efficiency	Inhibition Constant (Ki)	Intermol Energy	Lipophilic Evdw	Electroststic Energy	Total Internal	Torsional Energy
Remdesivir	-4.83	-0.12	285.72	-8.03	-7.95	-0.09	-1.47	4.66
R1	-5.15	-0.1	168.77	-8.59	-8.46	-0.13	-1.5	4.94
R2	-6.68	-0.12	12.61	-8.99	-8.82	-0.16	-3.46	5.76
R3	-8.85	-0.17	326.27	-8.48	-8.4	-0.08	-5.58	5.21
R4	-6.67	-0.12	12.98	-7.44	-7.37	-0.07	-4.44	5.21
R5	-6.25	-0.12	26.27	-8.22	-8.13	-0.09	-3.25	5.21
R6	-5.74	-0.11	61.76	-7.13	-7.21	0.09	-3.83	5.21
R7	-6.67	-0.12	12.87	-7.94	-7.94	0	-4.22	5.49
R8	-4.71	-0.09	352.02	-8.45	-8.34	-0.11	-1.75	5.49
R9	-10.04	-0.19	43.6	-9.01	-9.19	0.19	-6.25	5.21
R10	-6.79	-0.13	10.62	-7.59	-7.56	-0.03	-4.41	-5.21
R11	-6.06	-0.11	36.17	-8.52	-8.57	0.06	-2.75	5.21
R12	-5.88	-0.11	48.59	-6.86	-6.9	0.05	-4.24	5.21
R13	-5.69	-0.11	67.12	-8.1	-8.06	-0.04	-2.81	5.21
R14	-7.51	-0.14	3.11	-8.68	-8.64	-0.03	-4.05	5.21
R15	-7.85	-0.15	1.75	-6.6	-6.74	0.15	-6.47	5.21
R16	-6.51	-0.12	16.99	-6.21	-6.18	-0.03	-5.79	-5.49
Ligand (α-ketoamide)	-7.36	-0.17	4.05	-10.03	-10.05	0.02	-1.17	3.84

Table 3: No. of hydrogen and hydrophobic bond with bond length and p-p interaction of RDV, α-ketoamide and analogs

Analogs	No. of hydrogen bonding	H-bonds Amino Acid involve with bond length	No. of hydrophobic bond	Hydrophobic bonding	pi-Stacking
RDV	3	Tyr54 (2.70), Tyr54 (2.30), Glu166 (2.22)	1	Phe140 (3.96)	His 41
α-ketoamide	3	His41 (2.54), Gly143 (2.58), Glu166 (2.54)	5	His41 (3.52), His164 (3.95), Met165 (3.67), Glu166 (3.85), Asp187 (3.31)	
R1	2	Asn142 (2.6), Glu166 (2.41)	1	Thr25 (3.10)	
R2	6	Glu166 (3.46), Arg188 (3.33), Arg188 (2.58), Gln189 (3.45), Thr190 (3.27), Gln192 (3.69)	2	Thr25 (3.88), Glu166 (3.44)	His 41
R3	6	Asn142 (2.66), Asn142 (2.03), Glu166 (2.56), Gln189 (2.67), Gln189 (3.31), Thr190 (3.05)	2	Met165 (3.69), Asp187 (3.66)	His 41
R4	2	His164 (2.07), Glu166 (3.04)	2	Met165 (3.70), Glu166 (3.50)	
R5	2	Gly143 (2.03), Gln189 (2.76)	3	Phe140 (3.60), Met165 (3.69), Glu166 (3.33)	
R6	5	Arg188 (2.54), Gln189 (3.03), Thr190 (3.01), Thr190 (2.84), Gln192 (2.59)	2	Glu166 (3.54), Pro168 (3.99)	
R7	2	Glu166 (2.94), Gln189 (2.05)	2	Leu167 (3.34), Gln192 (3.55)	
R8	5	Thr26 (2.05), Glu166 (2.18), Gln189 (2.88), Asn142 (3.23), Gln192 (3.30)	4	Thr25 (3.45), Met165 (3.41), Pro168 (3.92), Asp187(3.83)	
R9	6	His164 (2.16), Glu166 (2.07), Glu166 (2.70), Gly170 (3.11), Thr190 (3.15), Gln192 (2.95)	2	Pro168 (3.30), Pro168 (3.82)	His 41
R10	3	Arg188 (3.38), Gln189 (2.65), Gln192 (3.15)	3	Met165 (3.29), Glu166 (3.74), Gln189 (3.81)	

Continue…

R11	3	Thr26 (2.14), Asn142 (2.73), Gln189 (3.69)	3	Met165 (3.54), Pro168 (3.55), Gln192 (3.77)	
R12	5	Glu166 (2.93), Arg188 (3.15), Arg188 (2.37), Thr190 (3.10), Gln192 (3.18)	2	Glu166 (3.77), Gln189 (3.49)	
R13	3	Asn142 (3.04), Gly143 (2.69), Glu166 (3.93)	3	Thr25 (3.85), Leu141 (3.59), Glu166 (3.65)	
R14	4	Gly143 (3.04), Glu166 (2.87), Gln192 (3.18)	2	Phe140 (3.51), Glu166 (3.73)	
R15	5	Asn142 (3.39), Glu166 (2.91), Glu 166 (3.26), Thr190 (2.55), Gln192 (3.11)	1	Glu166 (3.20)	
R16	5	Asn142 (3.37), Glu166 (2.40), Gln189 (3.16), Thr190 (2.95), Gln192 (2.24)	1	Gln189 (3.45)	

nm and R15 was 1.1163nm. The plot of RMSD indicates stable curves for all selected ligand-protein complexes during the simulation time that was 500ps. This result clearly shows that ligands were stable inside the pocket and don't change their orientation in the active site.

The RMSF values were calculated for each residue and the fluctuation from its average position gives insight into the flexibility of regions of active site of protein. The RMSF results show that the fluctuations per residue are higher in three different reagions that are amino acids 44-70, 118-169, 188-194 and in addition to 220 to 284. It is indicated that these residues are participating in the ligand binding. The average values of RMSF of R3, R9, R14 and R15 were 0.6680nm, 0.6923nm, 0.7312nm and 0.7283nm respectively.

CONCLUSION

In the present research study, we described the designing of remdesivir analogs and their docking with the receptor. The study uncovered the binding behavior of the drug and analogs. It was observed that the α-ketoamide, RDV, and analogs were bound with specific amino acids (that were Thr^{25}, His^{41}, Tyr^{54}, Asn^{142}, Gly^{143}, Cys^{145}, His^{164}, Glu^{166}, Asp^{187}, Gln^{189}, Thr^{190} and Gln^{192}) of the receptor. The binding energy was in the range of -10.08kcal/mol to -4.71kcal/mol. The deep study of SAR revealed that the analogs having sulfur group and bromo-group bind more strongly with the target as compared to the analogs which have amino-group in their structure. The analog R3, R9, R14 and R15 were evaluated as the best docked compounds among all and there stability was check by MD simulation by mean of RMSD. It was observed that the all selected compounds were stable in the binding pocket without altering protein native structures during 500ps. Furthermore, the analog R9 can be a lead compound for futher *In vitro* and *In vivo* activity studies.

REFERENCES

Al-Tannak NF, Novotny L, Alhunayan A (2020). Remdesivir-bringing hope for COVID-19 treatment. *Sci. Pharm.,* **88**(2): 29.

Anand K, Palm GJ, Mesters JR, Siddell SG, Ziebuhr J and Hilgenfeld R (2002). Structure of coronavirus main proteinase reveals combination of a chymotrypsin fold with an extra alpha-helical domain. *EMBO J.*, **21**(13): 3213-3224.

Bacha U, Barrila J, Velazquez-Campoy A, Leavitt SA and Freire E (2004). Identification of novel inhibitors of the SARS coronavirus main protease 3CLpro. *Biochem.*, **43**(17): 4906-4912.

Brooks BR, Brooks 3rd CL, Mackerell Jr AD, Nilsson L, Petrella RJ and Roux B, Won Y, Archontis G, Bartels C, Boresch S, Caflisch A, Caves L, Cui Q, Dinner AR, Feig M, Fischer S, Gao J, Hodoscek M, Im W, Kuczera K, Lazaridis T, Ma J, Ovchinnikov V, Paci E, Pastor RW, Post CB, Pu JZ, Schaefer M, Tidor B, Venable RM, Woodcock HL, Wu X, Yang W, York DM and Karplu M (2009). CHARMM: The biomolecular simulation program. *J. Comput. Chem.,* **30**(10): 1545-1614.

Cao Y, Deng QX and Dai SX (2020). Remdesivir for severe acute respiratory syndrome coronavirus 2 causing COVID-19: An evaluation of the evidence. *Travel Med Infect Dis.*, **35**: 101647.

ChemOffice (2009). ChemOffice 6.0 Trial Version, http:// www.cambridgesoft.com.

Dassault Systèmes BIOVIA (2017). Discovery Studio Modeling Environment, Release. Dassault Systèmes; San Diego, CA, USA.

Darden T, York D and Pedersen L (1993). Particle mesh Ewald: An N·log (N)method for Ewald sums in large systems. *J. Chem. Phys.,* **98**(12): 10089-10092.

Eastman RT, Roth JS, Brimacombe KR, Simeonov A, Shen M, Patnaik S and Hall MD (2020). Remdesivir: A review of its discovery and development leading to emergency use authorization for treatment of COVID-19. *ACS Cent. Sci.,* **6**(5): 672-683.

Elfiky AA (2020) Ribavirin, Remdesivir, Sofosbuvir, Galidesivir and Tenofovir against SARSCoV-2 RNA dependent RNA polymerase (RdRp): A molecular docking study, *Life Sci.,* **15**(253): 117592.

Elfiky AA (2020) SARS-CoV-2 RNA dependent RNA polymerase (RdRp) targeting: An in silico perspective.

J. Biomolec Struct Dyna. https://doi.org/10.1080/07391102.2020.1761882)

Fung TS and Liu DX (2019). Human coronavirus: Host-pathogen interaction. *Annu. Rev. Microbiol.,* **73**: 529-557.

Humphrey W, Dalke A and Schulten K (1996). VMD: Visual molecular dynamics. *J. Mol. Graph.,* **14**(1): 33-38 27-8.

Jorgensen WL, Chandrasekhar J, Madura JD, Impey RW and Klein ML (1983). Comparison of simple potential functions for simulating liquid water. *J. Chem. Phys.,* **79**(2): 926-935.

Koulgi S, Jani V, Uppuladinne MVN, Sonavane U and Joshi R (2020). Remdesivir-bound and ligand-free simulations reveal the probable mechanism of inhibiting the RNA dependent RNA polymerase of severe acute respiratory syndrome coronavirus. *RSC Adv.,* **10**(45): 26792.

Kumar Y, Singh H and Patel CN (2020). *In silico* prediction of potential inhibitors for the main protease of SARS-CoV-2 using molecular docking and dynamics simulation based drug-repurposing. *J. Infect. Public Health,* **13**(9): 1210-1223.

MacKerell AD, Bashford D, Bellott M, Dunbrack RL, Evanseck JD, Field MJ, Fischer S, Gao J, Guo H, Ha S, Joseph-McCarthy D, Kuchnir L, Kuczera K, Lau FTK, Mattos C, Michnick S, Ngo T, Nguyen DT, Prodhom B, Reiher WE, Roux B, Schlenkrich M, Smith JC, Stote R, Straub J, Watanabe M, Wiórkiewicz-Kuczera J, Yin D, and Karplus M (1998). All-atom empirical potential for molecular modeling and dynamics studies of proteins. *J. Phys. Chem. B.,* **102**(18): 3586-3616.

Pastor RW, Brooks BR and Szabo A (1988). An analysis of the accuracy of Langevin and molecular dynamics algorithms. *Mol. Phys*., **65**(6): 1409-1419.

Pizzorno A, Padey B, Julien T, Assant ST, Traversier A, Cerda EE, Fouret J, Dubois J, Gaymard A, Lescure FX, Dulière V, Brun P, Constant S, Poissy J, Lina B, Yazdanpanah Y, Terrier O and Calatrava MR (2020). Characterization and treatment of SARSCoV-2 in nasal and bronchial human airway epithelia. *Cell reports Med.,* **1**(4): 100059.

PyMOL; The PyMOL Molecular Graphics System, Version 2.0 Schrodinger, LLC.

Salentin S, Schreiber S, Haupt VJ, Adasme MF, Schroede M (2015). PLIP: Fully automated protein-ligand interaction profiler. *Nucl. Acids Res.,* **43**(W1): W443-W447.

Shannona A, Lea TTL, Seliskoa B, Eydouxa C, Alvareza K, Guillemots JC, Decrolya E, Peersenb O, Ferrona F, Canarda B (2020). Remdesivir and SARS-CoV-2: Structural requirements at both nsp12 RdRp and nsp14 Exonuclease active-sites. *Anti Res.,* **178**(Issue): 104793

Sheahan TP, Sims AC, Leist SR, Schäfer A, Won J, Brown AJ, Montgomery SA, Hogg A, Babusis D, Clarke MO, Spahn JE, Bauer L, Sellers S, Porter D, Feng JY, Cihlar T, Jordan R, Denison MR, Baric RS . (2020). Comparative therapeutic efficacy of remdesivir and combination lopinavir, ritonavir, and interferon beta against MERSCoV. *Nat. Commun.,* **11**(Issue): 222.

Trott O and Olson AJ (2010). Auto Dock Vina: Improving the speed and accuracy of docking with a new scoring function, efficient optimization, and multithreading. *J. Comput. Chem.*, **31**(2): 455-461.

Wang M, Coa R, Zhang L, Yang X, Liu J, Xu M, Shi Z, Hu, Z, Zhong W and Xiao G (2020) Remdesivir and chloroquine effectively inhibit the recently emerged novel coronavirus (2019-nCoV) *in vitro*. *Cell Res*., **30**(3): 269-271.

Williamson BEN, Feldmann F and Schwarz B Meade-White K, Porter DP, Schulz J, Doremalen NV, Leighton I, Yinda CK, Pérez-Pérez L, Okumura A, Lovaglio J, Hanley PW, Saturday G, Bosio CM, Anzick S, Barbian K, Cihlar T, Martens C, Scott DP, Munster VJ, and Wit ED (2020). Clinical benefit of remdesivir in rhesus macaques infected with SARSCoV-2. *Nature,* 585 (issue) 273-276.

Wrapp D, Wang N, Corbett KS, Goldsmith J A, Hsieh CL, Olubukola A (2020). Cryo-EM structure of the 2019-nCoV spike in the prefusion conformation. *Bio. Rxiv*., **367**(6483): 1260-1263.

Xu X, Ping Chen P, Jingfang Wang J, Feng J, Zhou H, Xuan Li X, Zhong W, Hao P (2020). Evolution of the novel coronavirus from the ongoing Wuhan outbreak and modeling of its spike protein for risk of human transmission. *Sci. China Life Sci*., **63**(3): 457-460.

Zhang L, Lin D, Sun X, Curth U, Drosten C, Sauerhering L, Becker S, Rox K and Hilgenfeld R (2020). Crystal structure of SARS-CoV-2 main protease provides a basis for design of improved α-ketoamide inhibitors. *Sci.,* **368**(6489): 409-412.

Zhang XW and Yap YL (2004). Old drugs as lead compounds for a new disease? Binding analysis of SARS coronavirus main proteinase with HIV, psychotic and parasite drugs. *Bioorg Med Chem.*, **12**(10): 2517-2521.